https://doi.org/10.5194/egusphere-2023-1858
Preprint. Discussion started: 5 September 2023

Geographic variability of dust and temperature in climate scaling regimes over the Last Glacial Cycle.

Nicolás Acuña Reyes[1], Elwin van 't Wout[1], Fabrice Lambert[2], and Shaun Lovejoy[3]

[1]Institute for Mathematical and Computational Engineering, School of Engineering and Faculty of Mathematics, Pontificia Universidad Católica de Chile
[2]Geography Institute, Pontificia Universidad Católica de Chile
[3]Physics Department, McGill University

Correspondence: Nicolás Acuña Reyes (nmacuna@uc.cl)

Abstract. Temperature and mineral dust records serve as valuable paleoclimate indicators for studying atmospheric variability across a wide range of temporal scales. Due to the typically lower resolution of older sections within these records, studies investigating the geographical variability of the atmosphere have predominantly focused on periods shorter than one glacial cycle, such as the Holocene or the Last Glacial Maximum. In this study, we utilise a Haar-based algorithm to evaluate the geographic variability of dust and temperature records throughout the last glacial cycle. This algorithm enables us to analyse non-equidistant sampling series, allowing for the utilisation of both high and low-frequency information from the records. Consequently, we can investigate timescales ranging from decades to thousands of years. Notably, our findings indicate that the transition from macroweather to climate regimes occurs at shorter timescales in polar regions compared to the tropics or mid-latitudes. Furthermore, disparities between the dust records of the North and South Poles were observed. Finally, we assess the time-dependent correlation between the polar regions and the lower latitudes. Our analysis reveals high correlations at timescales of approximately 20, 40, and 100 kyr, which aligns with the Milankovitch cycles. Conversely, all sites exhibit a loss of correlation between 40 and 80 kyr, indicating the absence of an identifiable oscillation synchronisation mechanism at these scales. On the one hand, our findings support the use of the Haar-based method as an alternative for analysing nonuniform datasets. On the other hand, they underscore the necessity for additional high-resolution or longer time series data from the tropics or mid-latitudes, as the currently available data fail to adequately represent the glacial-interglacial cycles.

1 Introduction

The study of paleoclimate, which involves reconstructing past climate variations using various paleoclimatic archives, provides crucial insights into understanding Earth's climatic history (Ruddiman, 2008). Paleoclimatic archives, such as ice cores and sedimentary records, offer unique opportunities to investigate climate dynamics on various timescales, ranging from annual to millennial and beyond (North Greenland Ice Core Project members et al., 2004). These archives preserve information about past changes in air and sea temperature, atmospheric aerosol content, precipitation regimes, etc., enabling researchers to discern patterns and drivers of climate variability over extended periods (von der Heydt et al., 2021).

https://doi.org/10.5194/egusphere-2023-1858
Preprint. Discussion started: 5 September 2023

Understanding the temporal complexity of paleoclimate records has been a long-standing challenge in climate science. The inherent non-linear and chaotic nature of Earth's climate system often leads to multifaceted interactions and feedback mechanisms acting over a wide range of scales. Conventional statistical methods, while essential, may not fully capture the intricate dynamics within paleoclimatic timeseries, leaving significant patterns undiscovered. Furthermore, because of the many different physical processes interacting within the climate system, its variability spectrum is far from being composed of pure spikes belonging to a well-defined forcing process such as daily variations or Milankovich cycles. Instead, the bulk of the spectrum is, in fact, continuous and scales over large ranges. Moreover, it is shown in Wunsch (2003) that the quasiperiodic signals represent only a small fraction of the total variability.

Research that delves into climate variability across various scales has revealed that dynamical atmospheric regimes are characterised by scaling. Notably, over the past 540 million years (the Phanerozoic eon), five distinct scaling regimes have been identified (Lovejoy, 2023). These are the weather regime (spanning from 6 hours up to 20 days), the macroweather regime (covering 20 days to 50 years), the climate regime (encompassing 50 years to 80 kyr), the macroclimate regime (ranging from 80 to 500 kyr), and the megaclimate regime (denoting time scales larger than 500 kyr). Here, the macroweather and climate regimes hold particular significance due to their intricate interaction and overlap with anthropogenic forcing. In the macroweather regime, Lovejoy (2015) suggest that beyond about ten days, average fluctuations over longer times tend to smaller values and therefore converge towards an average state. In contrast, fluctuations in the climate regime start to increase with scale from some critical time scale τ_c, becoming more and more divergent and leading to the large glacial-interglacial variability. Therefore, a key issue for understanding macroweather and climate variability is the determination of τ_c.

Over the past decade, numerous studies have focused on scaling in paleoclimatic data (e.g., Fredriksen and Rypdal, 2016; Laepple and Huybers, 2013; Lovejoy and Varotsos, 2016; Nilsen et al., 2016). Some of these studies evaluated how well climate models reproduce observed long-term climate variability (e.g., Zhu et al., 2019). While climate models and reconstructions show reasonable consistency on seasonal to interannual time scales, significant discrepancies emerge at longer time-scales and at regional scales, with models underestimating the variability (Laepple and Huybers, 2014). However, due to the low number and resolution of long paleoclimatic time series, these studies typically focus on timescales shorter than a glacial cycle and longer spatiotemporal patterns are not yet well understood. As a result, analysing the spatial distribution of τ_c (transition time scale) is a significant component for an improved comprehension of the temporal and spatial structures of climate variability.

In this study, we used Haar wavelets to analyse global spatiotemporal atmospheric variability over the last glacial cycle, as Haar-based methods are a convenient choice for accurately estimating scaling exponents (Lovejoy and Schertzer, 2012). For this purpose, we selected temperature and dust data based on both its duration and resolution. These records usually have non-equidistant sampling rates and rapidly lose resolution as we move to older time sections, limiting high-frequency analyses. Pre-processing techniques such as linear interpolation can convert non-uniform data resolution to uniform time series, but this always implies some high-frequency information loss, which is essential for finding scaling transitions. In this paper, we extend the Haar fluctuation analysis to non-uniform time series, allowing us to work with long non-uniform datasets and characterise climate variability over a wider range of regimes, from decadal to multi-millennial timescales.

https://doi.org/10.5194/egusphere-2023-1858
Preprint. Discussion started: 5 September 2023

Because the climate involves many intimately coupled processes, understanding variability at any one timescale requires some understanding of the whole (Huybers and Curry, 2006). Hence, we also used our non-uniform Haar fluctuation algorithm to quantify the correlations between different datasets as a function of timescale. In particular, we compared the Arctic-Antarctic cross-Haar correlation with the correlations between the poles and mid-latitude sites. Finally, we also compared the correlation between dust and temperature records when available at the same site. Our study of paleoclimatic archives gives improved insight into the interconnection behind climate processes and records.

2 Datasets description

We use paleoclimatic records of both temperature and dust, based on isotope measurements for the former, and direct particle measurements for the latter. These records were obtained from marine sediment cores, ice cores, loess deposits and lake sediments. Only a few sites have records of both temperature and dust, perhaps at different resolution. However, only one of the two variables was reconstructed in most sites. Since we are specifically interested in covering the macro-weather and climate regimes, we mostly included paleoclimatic archives that cover at least the past 50,000 years at centennial resolution or better in our analysis. Figure 1 and Table 1 show the location and characteristics of each record included in this study.

Most sites are located in the polar regions such as Greenland and Antarctica, where measuring proxies at high temporal resolution is easier to achieve than in the tropics and at mid-latitudes. Unfortunately, no datasets that satisfy our selection criteria were available in regions such as Central and South America, South Asia, and Australia. Some datasets covered multiple glacial cycles, such as the EPICA Dome C records or the Xifeng loess archive, whereas other records extend only a single glacial-interglacial cycle or less. To avoid mixing information from multiple glacial cycles, we restricted the analysis to the most recent 130 kyr (roughly the last glacial-interglacial cycle).

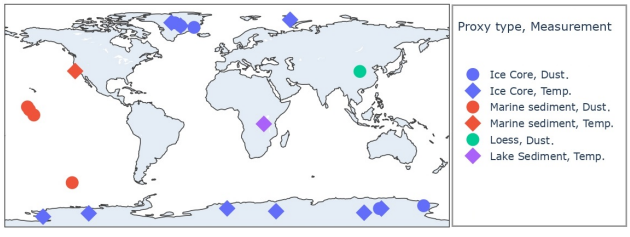

Figure 1. The global distribution of the datasets included in this study. The temperature and dust flux records come from ice cores, loess, lake and marine sediments.

Paleoclimate archives rarely have a uniform resolution since each data point correspond to a thin layer of core material that may correspond to a different time span than other layers. Figure 2 shows the proportion of age covered within the time duration for each dataset. Notice that a uniform dataset has a linear relation, but most curves are above the diagonal, indicating a higher resolution at early samples and lower resolution at older samples. We observe that the sampling rates depend on the specific dataset and most are significantly non-uniform.

https://doi.org/10.5194/egusphere-2023-1858
Preprint. Discussion started: 5 September 2023

Table 1. Summary of the datasets.

Data id	Name	Latitude (°)	Longitude (°)	Proxy type	Span (ky)	Resolution (y)	Unit	Reference
			Dust measurements					
1	EDC	-75.10	123.35	Ice core	130	1	mg/m^2/y	(Lambert et al., 2012)
2	Talos Dome	-72.82	159.18	Ice core	150	2	μg/kg	(Schüpbach et al., 2013)
3	Central South Pacific	-54.22	-125.43	Marine sediment	474	199	wt-%	(Lamy et al., 2014)
4	Central Pacific Ocean 1 (17PC)	0.48	-156.45	Marine sediment	149	756	g/m^2/y	(A.Jacobel et al., 2016)
5	Central Pacific Ocean 2 (31BB)	4.68	-160.05	Marine sediment	141	531	g/m^2/y	(A.Jacobel et al., 2016)
6	Central Pacific Ocean 3 (37BB)	7.04	-161.63	Marine sediment	144	1,319	g/m^2/y	(A.Jacobel et al., 2016)
7	Xifeng - China	35.70	107.60	Loess	800	1,108	g/m^2/ky	(Guo et al., 2009)
8	RECAP	71.30	-26.72	Ice core	121	66	μg/kg	(Simonsen et al., 2019)
9	GRIP	72.59	-37.64	Ice core	248	79	μg/kg	(De Angelis and Legrand, 1994)
10	NGRIP	75.00	-42.30	Ice core	108	36	μg/kg	(Ruth et al., 2007b)
			Temperature measurements					
11	WAIS	-79	-112	Ice core	68	11	δO18 (per mil)	(Buizert et al., 2015)
12	Vostok	-78.46	106.87	Ice core	423	128	δD (%SMOW)	(Petit et al., 1999)
13	Dome Fuji	-77.3	39.7	Ice core	340	286	δO18 (per mil)	(Sato et al., 2013)
14	EPICA EDML	-75.00	0.07	Ice core	150	65	δO18 (%SMOW)	(Ruth et al., 2007a)
15	EDC	-75.1	123.35	Ice core	801	138	δD (per mil)	(Jouzel et al., 2007)
16	Lake Tanganyika - Eastern Africa	-6.65	29.80	Lake sediment	59	280	°C	(Tierney et al., 2008)
17	Central California	37	-123	Marine sediment	161	594	δO18 (per mil)	(Lyle et al., 2010)
18	GRIP	72.59	-37.64	Ice core	104	21	δO18 (%SMOW)	(Seierstad et al., 2014)
19	NGRIP	75.1	-42.3	Ice core	123	20	°C	(Seierstad et al., 2014)
20	NEEM	77.45	51.06	Ice core	111	5	δO18 (%SMOW)	(Gkinis et al., 2021)

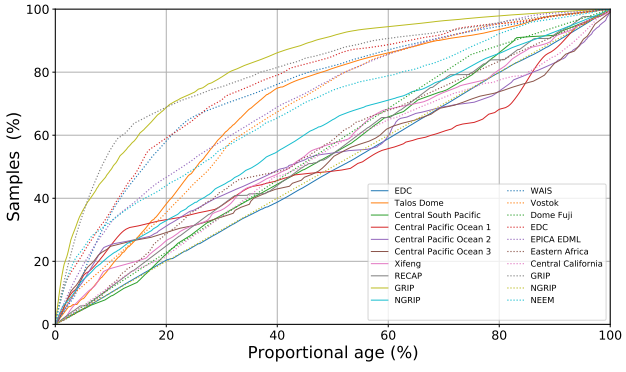

Figure 2. The proportion of samples covered within the first part of the age. The continuous lines depict dust datasets while the dotted lines depict temperature datasets.

As an example of a dataset for this study, Figure 3 shows the most recent 130 kyr of four dust and temperatures ice core time series. The plots clearly show the highly spiky nature of the data.

https://doi.org/10.5194/egusphere-2023-1858
Preprint. Discussion started: 5 September 2023

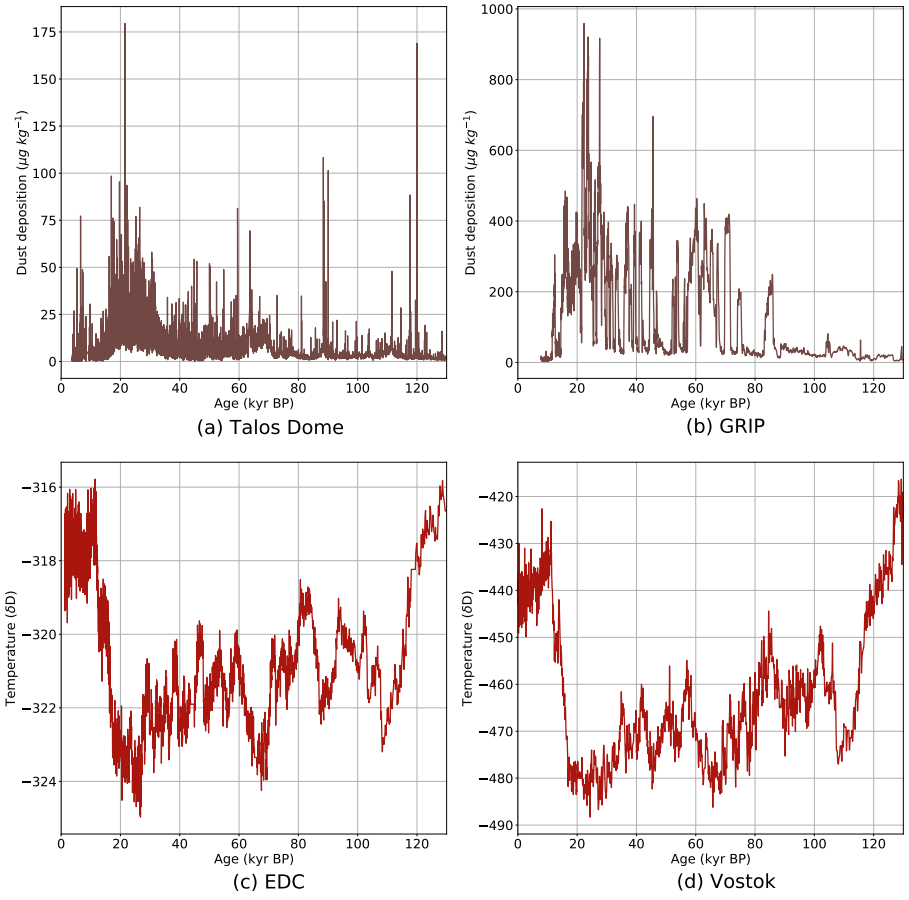

Figure 3. Several examples of the dust and temperature ice cores time series. The upper row shows the dust flux from (a) Talos Dome and (b) GRIP. The lower row displays temperatures from (c) Epica Dome C and (d) NGRIP.

3 Methodology

This study aims to analyse the climate scaling regimes from paleoclimate data, which tend to have non-equidistant samples and many spikes. Algorithms based on Fourier transforms have low accuracy for nonuniform and spiky data. In fact, we applied a nonuniform FFT algorithm to the data but the scaling regimes were not clearly visible from the analysis. Hence, we use Haar fluctuation analysis (Lovejoy and Schertzer, 2012), which was adapted to nonuniform data as in Lovejoy (2015). The Haar fluctuations are more robust against spikes in the data and better suited to show different scaling regimes. Furthermore, no pre-processing of the data, such as normalization and outlier filtering, was necessary for the Haar analysis. The only preprocessing step we performed was removing the sample mean from the time series before computing the cross-Haar correlations.

https://doi.org/10.5194/egusphere-2023-1858
Preprint. Discussion started: 5 September 2023

3.1 Haar wavelets and fluctuations

The Haar wavelet analysis is a powerful technique to characterize timescale-dependent variability in a time series $F(t)$. The Haar fluctuation has a simple definition and the results have a clear interpretation. Furthermore, it can be extended to irregular sampling rates, thus avoiding data preprocessing such as interpolation between time samples. Hence, the algorithm uses all information available from the data, also on the shorter timescales represented by sections with high resolution.

The Haar wavelet is a piecewise constant function that is used as shape function in fluctuation analysis. The Haar fluctuation ΔF over a uniform time interval Δt is defined as the absolute difference of the mean over the first and second halves of an interval, that is,

$$\Delta F(\Delta t) = \frac{1}{\frac{\Delta t}{2}} \left(\int_{t-\Delta t}^{t-\Delta t/2} F(t')dt' - \int_{t-\Delta t/2}^{t} F(t')dt' \right). \tag{1}$$

When the Haar fluctuation over a range of timescales Δt obeys a power law relation ($\Delta F(\Delta t) \propto \Delta t^H$), then the mean absolute fluctuation also varies as

$$\langle |\Delta F(\Delta t)| \rangle \propto \Delta t^H, \tag{2}$$

where the brackets "$\langle\rangle$" indicate the sample mean over all available disjointed intervals of size Δt (fluctuation period) in the time series. Here, the exponent H characterizes the scaling regime, with $H > 0$ meaning that the average fluctuations increase with scale, while $H < 0$ implies the opposite. This fluctuation exponent estimation is appropriate within the range $H \in [-1, 1]$, which is valid for almost all geophysical data analysed to date (Lovejoy and Schertzer, 2012). A more general q-th moment of the fluctuations can be estimated by defining the "generalised structure functions" $S_q(\Delta t)$,

$$S_q(\Delta t) = \langle |\Delta F(\Delta t)|^q \rangle \propto \Delta t^{\xi(q)}, \tag{3}$$

where the exponent $\xi(q)$ is composed of a linear part and a non-linear ($K(q)$) part:

$$\xi(q) = qH - K(q). \tag{4}$$

3.2 Haar fluctuations on non-equidistant data

The definition of the Haar fluctuation in Equation (1) assumes a uniform timestep. Here, we follow Lovejoy (2015) appendix B and extend the Haar analysis to nonuniform time series, as necessary to accurately analyse the datasets in our study. First, let us assume there are N measurements of a process $T(t_i)$, where $(t_i)_{i\in[1,N]}$ are irregular time samplings. Then, we define the cumulative sum S_i as

$$S_i = \sum_{j \le i} T(t_j). \tag{5}$$

https://doi.org/10.5194/egusphere-2023-1858
Preprint. Discussion started: 5 September 2023

By taking an index j and an even number k, we can define $[t_j, t_{j+k}]$ as the interval where fluctuation $\Delta T_{j,k}$ will be estimated. To do so, we determine the sums of $T(t_i)$ over the first and second halves of the interval as:

$$\Delta S^{(1)} = S_{j+k/2} - S_j \quad , \quad \Delta S^{(2)} = S_{j+k} - S_{j+k/2}, \tag{6}$$

and compute the average of the first half minus the average of the second half of the $[t_j, t_{j+k}]$ interval as follows:

$$\Delta T_{j,k} = 2\left(\frac{\Delta S^{(1)}}{t_{j+k/2} - t_j} - \frac{\Delta S^{(2)}}{t_{j+k} - t_{j+k/2}}\right), \tag{7}$$

where the canonical factor 2 multiplying the difference is a calibration parameter necessary to expand the working range from anomaly ($H < 0$) and differences ($H > 0$) to the Haar range $-1 \leq H \leq 1$ (Lovejoy, 2023).

This definition works for any sampling rate but its accuracy deteriorates when the first and second halves of the interval cover very different time durations. Hence, we include a quality control on the uniformity of the intervals. For this purpose, we define the nonuniformity of the interval Δt by the ratio between time samples (ϵ) as

$$\epsilon = \frac{t_{j+k/2} - t_j}{t_{j+k} - t_j}. \tag{8}$$

Then, we define a threshold $\epsilon_{\min}$ and include only Haar fluctuations on intervals that satisfy $\epsilon_{\min} \leq \epsilon \leq (1 - \epsilon_{\min})$. Decreasing $\epsilon_{\min}$ implies a precision loss and hence it smooths the resulting curve. Differently, taking $\epsilon_{\min}$ too close to 1/2 (uniform sampling case) can result in the exclusion of too many fluctuations, with the consequence that the statistics will be poor. For this study, we fixed $\epsilon_{\min}$ at 1/4.

The first-order Haar structure function in Eq. (2) can readily be applied to our definition of nonuniform intervals. Furthermore, we can work with its second-order structure function to estimate the Haar fluctuation's root mean square (RMS) value as

$$\langle |\Delta F(\Delta t)|^2 \rangle^{1/2} \propto \Delta t^{\xi(2)/2} = \Delta t^{H - K(2)/2}, \tag{9}$$

as in Lovejoy and Lambert (2019). This statistic fully characterizes the scaling of Gaussian processes and gives important insights for non-Gaussian datasets. Thus, we will use the RMS fluctuation as an approximation to the absolute mean ($H \approx \xi(2)/2$) in the following.

3.3 Cross-Haar Correlation

So far, climate variability has been described by scaling relationships ($\Delta F(\Delta t) \propto \Delta t^H$) calculated by Haar fluctuations for a single time series. If the governing processes have consistent scaling patterns, we could expect interrelations between processes that lead to correlations. The correlations between two time series at different scaling regimes can be calculated with cross-Haar fluctuation analysis. This technique estimates the correlation between individual fluctuations at fixed time scales, that is, there is one correlation value at each Δt.

Let's consider two time series, denoted by $A(t)$ and $B(t)$, whose sample mean was removed, that is, $\langle \Delta A \rangle = \langle \Delta B \rangle = 0$. Furthermore, $\Delta A(\Delta t)$ and $\Delta B(\Delta t)$ denote the Haar fluctuations of A and B, respectively. Then, at the time lag Δt we can

https://doi.org/10.5194/egusphere-2023-1858
Preprint. Discussion started: 5 September 2023

compute the cross-Haar correlation as

$$\rho_{\Delta A,\Delta B}(\Delta t) = \frac{\langle \Delta A\ \Delta B \rangle}{\langle \Delta A^2 \rangle^{1/2} \langle \Delta B^2 \rangle^{1/2}}, \tag{10}$$

with the correlation coefficient $\rho_{\Delta A,\Delta B}(\Delta t) \in [-1, 1]$.

Since the time series likely have different sampling rates and duration, their fluctuations will cover different time scales which may not match each other, leading to an inaccurate estimation of ρ. To avoid this problem, we use linear interpolation to shift the sampling of the higher resolution series (say $A(t)$) and fit it with the sampling of the lower resolution one ($B(t)$) before computing its fluctuations. Shortening the duration of the time series to the maximum common Δt was also needed. Finally, since we end up with a cloud of fluctuations, we fit a cubic spline to simplify the visualisation.

4 Results

This section shows the computational results of the Haar fluctuation analysis on the various datasets. Section 4.1 shows the scaling regimes for individual sites, and the cross-correlations are presented in Section 4.2.

4.1 Haar fluctuation analysis

The Haar analysis yields a fluctuation RMS at each time lag, so that the scaling exponent H can be fitted for different regimes, as given by Equation (9). To analyze the spatial differences in scaling regimes, we clustered the measurement sites into five different groups according to latitude:

- Antarctica: From -90° to -60°.
- Southern mid-latitudes: From -60 to -20°.
- The tropics: From -20° to 20°.
- Northern mid-latitudes: from 20° to 60°.
- Arctic: From 60° to 90°.

As explained in Section 3.1, when the average fluctuations increase with scale ($H > 0$), they represent unstable behaviour, whereas when they decrease with scale ($H < 0$), they converges toward a mean state. These exponents are shown as the slope of the RMS values from the Haar fluctuation on a log-log plot. To identify various scaling regimes, we visually detected different sections with scaling behavior and fitted a linear segment to estimate the slope (H). Figure 4 shows the Haar fluctuations RMS at all sites.

Figure 4(a) shows the Haar fluctuation RMS from the Antarctic records. We observe consistent results, with similar scaling patterns at the different sites and between the dust and temperature proxies. The slopes of the reference lines indicate the presence of an $H < 0$ regime (macro-weather), and an $H > 0$ regime (climate), with a fluctuation minimum between time lags

https://doi.org/10.5194/egusphere-2023-1858
Preprint. Discussion started: 5 September 2023

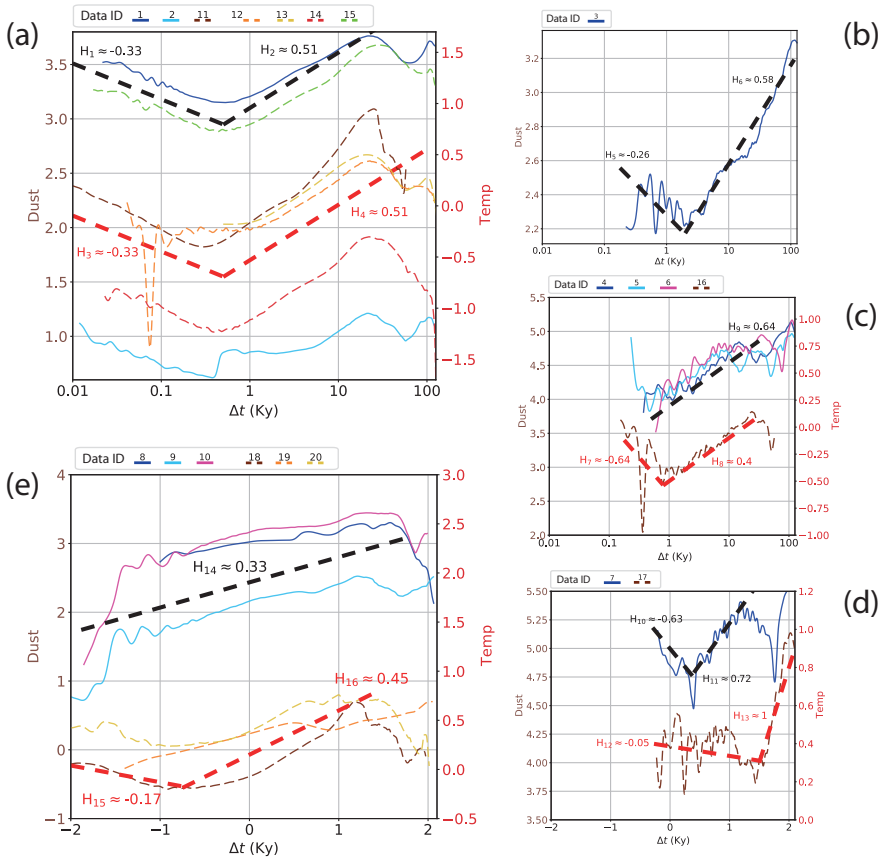

Figure 4. The curves depict Haar fluctuation RMS values at different scales, clustered by groups of sites with similar latitude: (A) Antarctic records, (B) Southern mid-latitudes records, (C) Tropics latitudes records, (D) Northern mid-latitudes records, and (E) Arctic records. Details of the sites can be found in Table 1. Units have been adapted to work within the same range. Dust proxies are displayed as continuous lines, whereas temperature proxies as dashed lines. Black (dust) and red (temperature) dashed lines were added as slope reference, together with the estimation of the H exponent.

of 310 and 560 years in all cases. This pronounced change in scaling regime shows that the macro-weather to climate transition (our estimate of τ_c) occurs at multi-centennial scales in the Antarctic. Furthermore, all datasets have a low-frequency peak somewhere between 17.8 to 31.6 kyr.

The Central South Pacific marine record is the only dataset located in the southern mid-latitudes. Figure 4(b) shows a minimum in Haar fluctuation RMS at timescales around 2 kyr. This suggests a macro-weather to climate transition (τ_c) at the millennial scale. Figure 4(c) shows fluctuations RMS from the Tropics, where we found differences between land and ocean variability. First, Lake Tanganyika presents a minimum at time lags around 580 years and a maximum around 25 thousands years, whereas the Central Pacific marine records show fluctuations that increase with scale but do not show any identifiable τ_c. Only ML1208-31BB (orange curve) shows a symmetry break at around Δt = 500 years. However, its slope on the short

https://doi.org/10.5194/egusphere-2023-1858
Preprint. Discussion started: 5 September 2023

timescales is less than the minimum detectable by Haar analysis ($H < -1$), so we cannot draw any confident conclusions. Similarly, the northern mid-latitudes do not show a consistent climate regime shift (see Figure 4(d)). On the one hand, a terrestrial record from Xifeng presents a minimum at timescales around 2 kyr and a peak around 18 thousands years. On the other hand, a marine record from Central California presents a large stable state during the macro-weather and climate regimes ($H_{12} \approx -0.05$), to eventually increase its variability around Δt = 31.6 kyr.

Finally, Figure 4(e) shows the Arctic Haar fluctuation RMS. Here, all temperature records except for NGRIP have a minimum at centennial scale, similar to the results from Antarctica. This suggests a climate regime change (τ_c) between Δt = 100 and 300 years. At the same time, the dust fluctuations present a completely different behaviour, with a sustained H exponent covering from multi-decadal to millennial scales ($H_{14} = 0.33$). At higher frequencies, the slope is larger than one and is thus out of the accurate range of Haar analysis. Therefore, it is not possible to identify a consistent climate regime transition for these records confidently. Table 2 summarises all Haar statistics at different latitudes.

Table 2. Climate regime transition summary. *Slope 1* denotes the H exponent found at decadal/centennial time scales (e.g., H_1, H_5, or H_7 in Figure 4), *Slope 2* denotes the H exponent found at centennial/millennial time scales (e.g., H_2, H_6, or H_8 in Figure 4), and τ_c correspond to the transition timescale from *slope 1* to *slope 2*.

Record	Slope 1	Slope 2	τ_c (y)
Arctic dust	>1	0.33	-
Arctic temp.	-0.17	0.45	100-300
Northern mid-latitudes Loess	-0.63	0.72	1,800-2,500
Northern mid-latitudes temp.	-0.05	1	-
Tropic dust	<-1	0.64	-
Tropic temp.	-0.64	0.4	580-1,000
Southern mid-latitudes dust	-0.26	0.58	1,800-2,000
Southern mid-latitudes temp.	-	-	-
Antarctica dust	-0.33	0.51	300-600
Antarctica temp.	-0.33	0.51	300-600

4.2 Haar correlation analysis

This section aims to analyze the interrelation between the poles and the lower latitudes. Using Haar fluctuations, we can estimate the time-dependent correlation coefficients pairwise, see Equation (10). Since almost all temperature records are from the poles, we excluded them from the analysis as we are mainly interested in the differences between the poles an the lower latitudes. Therefore, Figure 5 shows only the cross-Haar correlations of dust archives. Here, we estimated five pole-pole correlations (i.e., the correlation between Antarctic and Arctic records) and 15 pole-lower latitudes correlations. The light-blue and yellow areas highlight the pole-pole and the pole-lower latitudes correlations, respectively. Both cover one standard deviation from the mean, bounded to the upper limit of ρ = 1. We considered the RECAP-Central Pacific Ocean relationship an outlier (brown curve in Figure 5), and therefore excluded it from the bandwidth estimation.

https://doi.org/10.5194/egusphere-2023-1858
Preprint. Discussion started: 5 September 2023

Four main features can be highlighted in Figure 5. First, all records are uncorrelated at high frequencies, where local processes and noise probably dominate the variability. Second, the correlation of polar records rises quickly with scale, reaching ρ = 0.75 for periodicities of less than ten thousand years and staying strongly correlated ($\rho > 0.75$) throughout longer time scales. Third, polar records also start becoming correlated with lower latitude records as periodicity increases, but at a slower pace and never reaching the levels of pole-pole correlations. Specifically, it reaches a maximum of ρ = 0.75 around Δt = 35 kyr. Fourth, the polar against lower latitudes correlation shows a significant drop from Δt = 40 to 80 kyr. This drop is visible for both the pole-pole and pole-lower latitudes correlations, but is much more pronounced in the latter case, even reaching negative correlations for some pairs. All pairs but the RECAP-Pacific Ocean 3 eventually reach a perfect and positive correlation (ρ = 1) at scales around 100,000 years.

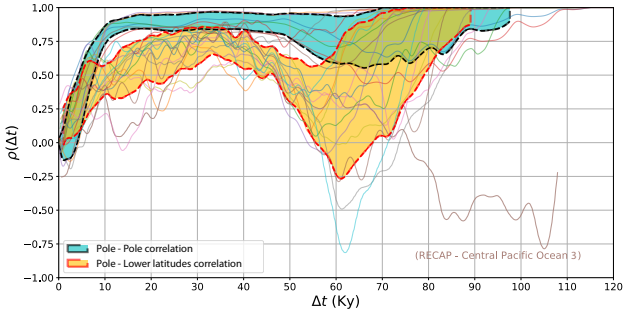

Figure 5. Cross-Haar fluctuation correlation of dust archives. The light-blue area highlights the Arctic-Antarctic correlation coefficients, whereas the yellow highlights the poles-tropics and pole-mid-latitude correlations. Both bands cover one standard deviation from the mean, in both directions.

Since both dust and temperature records were available for the EDC, GRIP, and NGRIP ice cores, we also analysed how these two variables are correlated within the same site. For this purpose, Figure 6 shows the cross-Haar correlation coefficient between dust and temperature measured in Antarctica (EDC records) and Greenland (GRIP and NGRIP records). The analysis shows no correlation at high frequencies, but the proxies quickly become anti-correlated at multimillennial timescales and longer, reaching ρ = -0.75 for periodicities shorter than 10,000 years in Greenland, and shorter than 20,000 years in Antarctica. All three sites show a drop in anti-correlation at Δt = 40 to 80 kyr, with significant differences between the three. All sites finally converge to ρ = -1, at timescales longer than Δt = 80 kyr.

5 Discussion

Paleotemperature and paleodust records are useful indicators to characterise atmospheric variability throughout a broad range of time scales. For an accurate study of climate scaling regimes, the datasets need to have sufficient length and resolution. On the one hand, we used records whose data length covers one or many glacial cycles, thus allowing past climate studies. On the other hand, their fine resolutions give high-frequency information, which is especially important to cover shorter climate regimes

https://doi.org/10.5194/egusphere-2023-1858
Preprint. Discussion started: 5 September 2023

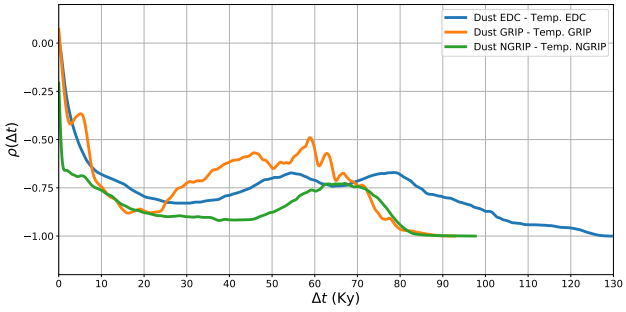

Figure 6. Same-site dust and temperature cross-Haar fluctuation correlations.

such as weather or macro-weather time scales. A major analysis issue is that the archives present time series with nonuniform sampling rates. Interpolation-based preprocessing typically utilises the mean resolution of the data to create uniform datasets, which can lead to high-frequency biases and information loss. Conversely, interpolation-free methods use the finer resolution information from the younger parts of the datasets, thus improving the accuracy of the variability estimator. Moreover, the sampling itself is scaling and can lead to important biases due to nonuniform data sampling in paleoseries. Further inquiries regarding this matter continue to be a work in progress.

In this study, we extended the Haar fluctuation analysis to nonuniform time series and calculated second-order Haar structure functions that characterise atmospheric variability across various timescales. Compared to other interpolation-free methods, the Haar structure function is one of the best algorithms since it gives more reliable estimates over a wide range of H, in particular $H \in [-1, 1]$ (Hébert et al., 2021; Lovejoy and Schertzer, 2012). At the same time, its definition and physical interpretation are straightforward since $H > 0$ means that the average fluctuations increase with scale, while $H < 0$ implies the opposite. A further advantage is that Haar fluctuations can be used to quantify the correlations between irregular series as a function of timescale. It is worth emphasising that, since the Haar function has a broad peak in the frequency domain, strong periodicity can make scaling hard to see. Hence, appropriate spectral analysis techniques can significantly enhance the Haar fluctuation analysis as complementary tools.

The Haar fluctuation analysis allows for detecting the τ_c parameter, which indicates the change from macro-weather to climate regimes. Our analysis showed that this regime change depends on latitude. While τ_c occurs at centennial to multi-centennial time scales in polar areas (Δt = 100-300 years in the Arctic, Δt = 300-600 years in Antarctica) it occurs at longer multi-centennial to millennial time scales at lower latitudes (Δt = 600-1000 years in the tropics, Δt = 1800-2500 years in the mid-latitudes). There are several caveats to this result, though. First, the tropical result is only from one terrestrial temperature record, while no macroweather - climate transition was detected in the tropical ocean dust records. Second, although the mid-latitudes result is consistent between terrestrial and marine dust records, a mid-latitude marine temperature record showed no macroweather - climate transition. Finally, the Greenland results are only derived from temperature data, with dust data showing no macroweather - climate transition.

https://doi.org/10.5194/egusphere-2023-1858
Preprint. Discussion started: 5 September 2023

It is only in Antarctica that all sites and both variables show consistent results. This may be due to the fact that all Antarctic sites are terrestrial, and both Antarctic temperature and dust are strongly affected by the same atmospheric processes (Markle et al., 2018). The results in polar dust and temperature show mostly the same signal at longer time scales (see discussion of Figure 6). It is striking that this relationship does not hold well in Greenland, where none of the dust records show the macroweather - climate transition suggested by the temperature records. Such differences at higher frequencies between the two suggests that the processes governing dust emission in East Asia and transport to Greenland over the Pacific and North America is strongly independent from the North Atlantic processes that govern temperature over Greenland at multi-decadal to multi-centennial time scales.

In the tropics and the mid-latitudes, a similar disengagement can be observed between dust and temperature records, as well as between marine and terrestrial records. However, in these cases the sites are so few and far apart that these differences are difficult to interpret. In addition, land and ocean differences are likely because the processes of climate recording and preservation are proxy-specific, thus single-proxy analysis should be preferred over mixed-proxy ones when possible (Reschke et al., 2021).

The cross-Haar correlation between dust records from different regions indicates that not only was the climatic variability consistent within polar areas, but also that the climatic variability between both poles is strongly linked. It is striking that the polar co-variability is established very quickly from multimillennial timescales onward. This suggests that Dansgaard-Oeschger (DO)/AIM events (EPICA Community Members et al., 2006) and orbital forcing, with their related ice sheet, vegetation, and oceanic circulation changes, are the main drivers of dust variability over long time scales. Polar - polar correlations are generally higher than the polar - lower latitudes correlations. This is due to polar amplification that increases the amplitude of variability in polar regions compared to the variability at lower latitudes.

The cross-Haar correlation between polar areas and lower latitudes is more nuanced. Like the polar - polar correlation, it starts with low values at high frequencies due to noise and independent local effects on dust variability. The link between polar areas and lower latitudes steadily increases towards multi-millennial time scales, to a first maximum around Δt = 20 to 40 kyr, which reflect the growing spatial influence of DO/AIM events, as well as precession and obliquity forcing. Furthermore, the 40 kyr scale is already influenced by the glacial cycle, as it is close to half of its period ($\sim$50 kyr). At eccentricity time scales (100,000 years) and beyond, the global correlation is also very high. There is a very interesting drop in correlation between the polar regions and the lower latitudes at time scales of Δt = 40 to 80 kyr, with a minimum around 60 kyr. This indicates that there is no internal forcing mechanism at work within the Earth system that would synchronise climate oscillations at a global spatial scale at these time scales.

The temperature on ice caps where ice cores are drilled is mainly a function of the height of the ice sheet, and the temperature of air masses reaching the drilling site, which themselves depend on ocean surface temperatures and atmospheric circulation (Masson-Delmotte et al., 2006). Recorded paleotemperature variability is therefore sensible to slow large-scale processes, such as ocean circulation changes (centennial to multi-centennial) and ice-sheet dynamics (millennial and multi-millennial). In contrast, dust deposition on polar ice sheets depends mainly on dust emissions at the source, washout efficiency during transport, and atmospheric circulation (Lambert et al., 2008). Recorded paleodust variability therefore is more sensible to

https://doi.org/10.5194/egusphere-2023-1858
Preprint. Discussion started: 5 September 2023

faster processes, such as wind speed and direction (annual to inter-annual), the hydrological cycle (annual to inter-annual), and terrestrial vegetation dynamics (decadal to multidecadal). Temperature and dust are anti-correlated because a colder atmosphere is drier, reducing washout, and also produces more sparse vegetation cover in source regions (Petit et al., 1999).

On longer time-scales, the slower processes will modulate changes in the faster processes (ice sheets and ocean currents will dictate the position of wind belts and the vegetation cover). Conversely, we expect the faster processes to decouple from the slow ones at shorter time-scales. This is visible in Figure 6, where dust and temperature are well-correlated at multi-millennial to orbital time-scales, but tend towards zero at shorter time-scales. It appears that dust and temperature become well-correlated ($\rho > 0.8$) only at multi-millennial time-scales, which suggests a predominant influence of the ice-sheets over ocean circulation changes on dust emissions and transport.

Similar to what was detected in the pole to lower latitude correlations, there is a drop in correlations in the band Δt = 40 to 80 kyr. Although the shape and maximum of the correlation drop varies a bit from record to record, the general explanation for it is the same: the orbital forcing synchronises the terrestrial, marine, and atmospheric processes at precession, obliquity, and eccentricity time-scales, while such a forcing is absent in the Δt = 40 to 80 kyr range, producing a decoupling of the ice-sheet and oceanic processes mainly influencing temperature, and the vegetation and atmospheric circulation processes mainly influencing dust.

6 Conclusions

In this study, we employed an extended the Haar fluctuation analysis approach to investigate scaling properties in various paleotemperature and paleodust records. Our findings underscore the rareness and significance of producing paleoclimatic datasets with both a large span and high temporal resolution. Through meticulous analysis of nonuniform time series, we identified the Haar structure functions as an effective tool to assess scaling properties of paleoclimatic time series, offering robust estimates across a wide range of Hurst exponent values. The Haar structure function's straightforward interpretation, tied to fluctuations' behaviour with scale changes, lends itself well to characterising climate transitions. In this study we presented an algorithm that performs Haar fluctuation analysis and cross-Haar correlations on non-equidistant time-series.

Our investigation into the τ_c parameter revealed latitudinal dependencies in the transition from macro-weather to climate regimes. We observe centennial to multi-centennial transitions in polar regions versus longer multi-centennial to millennial transitions at lower latitudes, highlighting the complex interplay between regional processes and global climatic influences. Furthermore, at longer scales, the parameter τ_c indicates a new prominent dominant forcing mechanism that doesn't align with Milankovitch's cycles, raising the question of what this mechanism might be.

The robust co-variability between polar sites underscores the pervasive impact of Dansgaard-Oeschger/AIM events and orbital forcing in polar areas. In contrast, the co-variability between polar regions and lower latitudes is less influenced by millennial scale events and more concentrated around the three orbital periodicities, with a distinct drop in correlation in the band between obliquity and eccentricity, highlighting the lack of global synchronising forcing in the Δt = 40 to 80 kyr range. This result is replicated in our cross-Haar correlation analysis of same-site temperature and dust records that shows a partial

https://doi.org/10.5194/egusphere-2023-1858
Preprint. Discussion started: 5 September 2023

decoupling of dust and temperature in this band, most probably due to different processes being at work in distant dust source areas and more proximal oceanic and ice-sheet processes.

In conclusion, our study demonstrates the power of extended Haar fluctuation analysis in unraveling the complexities of scaling in paleoclimatic time series. By elucidating the connections and disparities between various climate proxies, our findings contribute to a more comprehensive understanding of past climatic shifts and their underlying drivers across latitudinal and temporal dimensions.

Code and data availability. The data are available as supplement of the references listed in Table 1. A repository containing the Python function to estimate Haar fluctuations on non-equidistant datasets is available at https://github.com/NicoAcunaR/Non-equidistant_Haar_fluctuations.

Author contributions. All authors participated in the conceptualization of the research and the methodology. NA developed the software and visualization and conducted the formal analysis and investigation. EV, FL and SL provided supervision. NA prepared the original draft, and all authors contributed to reviewing and editing the final paper.

Competing interests. The authors declare that they have no conflict of interest.

Acknowledgements. This study was funded by ANID [Fondecyt 1231682 and 1221220].

https://doi.org/10.5194/egusphere-2023-1858
Preprint. Discussion started: 5 September 2023

References

A.Jacobel, J.McManus, R.Anderson, and G.Winckler: Large deglacial shifts of the Pacific Intertropical Convergence Zone, Nature Communications, https://doi.org/10.1038/ncomms10449, 2016.

Buizert, C., Adrian, B., Ahn, J., Albert, M., Alley, R. B., Baggenstos, Danieland Bauska, T. K., Bay, R. C., Bencivengo, B. B., Bentley, C. R., Brook, E. J., Chellman, N. J., Clow, G. D., Cole-Dai, J., Conway, H., Cravens, E., Cuffey, K. M., Dunbar, N. W., Edwards, J. S., Fegyveresi, J. M., Ferris, D. G., Fitzpatrick, J. J., Fudge, T. J., Gibson, C. J., Gkinis, V., Goetz, J. J., Gregory, S., Hargreaves, G. M., Iverson, N., Johnson, J. A., Jones, T. R., Kalk, M. L., Kippenhan, M. J., Koffman, B. G., Kreutz, K., Kuhl, T. W., Lebar, D. A., Lee, J. E., Marcott, S. A., Markle, B. R., Maselli, O. J., McConnell, J. R., McGwire, K. C., Mitchell, L. E., Mortensen, N. B., Neff, P. D., Nishiizumi, K., Nunn, R. M., Orsi, A. J., Pasteris, D. R., Pedro, J. B., Pettit, E. C., Buford Price, P., Priscu, J. C., Rhodes, R. H., Rosen, J. L., Schauer, A. J., Schoenemann, S. W., Sendelbach, P. J., Severinghaus, J. P., Shturmakov, A. J., Sigl, M., Slawny, K. R., Souney, J. M., Sowers, T. A., Spencer, M. K., Steig, E. J., Taylor, K. C., Twickler, M. S., Vaughn, B. H., Voigt, D. E., Waddington, E. D., Welten, K. C., Wendricks, A. W., White, J. W. C., Winstrup, M., Wong, G. J., and Woodruff, T. E.: Precise interpolar phasing of abrupt climate change during the last ice age, Nature, 520, 661–665, https://doi.org/10.1038/nature14401, 2015.

De Angelis, M. and Legrand, M.: Origins and variations of fluoride in Greenland precipitation, Journal of Geophysical Research: Atmospheres, 99, 1157–1172, https://doi.org/10.1029/93JD02660, 1994.

EPICA Community Members, Barbante, C.and Barnola, J.-M., Becagli, S., Beer, J., Bigler, M., Boutron, C., Blunier, T., Castellano, E., Cattani, O., Chappellaz, J., Dahl-Jensen, D., Debret, M., Delmonte, B., Dick, D., Falourd, S., Faria, S., Federer, U., Fischer, H., Freitag, J., Frenzel, A., Fritzsche, D., Fundel, F., Gabrielli, P., Gaspari, V., Gersonde, R., Graf, W., Grigoriev, D., Hamann, I., Hansson, M., Hoffmann, G., Hutterli, M. A., Huybrechts, P., Isaksson, E., Johnsen, S., Jouzel, J., Kaczmarska, M., Karlin, T., Kaufmann, P., Kipfstuhl, S., Kohno, M., Lambert, F., Lambrecht, A., Lambrecht, A., Landais, A., Lawer, G., Leuenberger, M., Littot, G., Loulergue, L., Lüthi, D., Maggi, V., Marino, F., Masson-Delmotte, V., Meyer, H., Miller, H., Mulvaney, R., Narcisi, B., Oerlemans, J., Oerter, H., Parrenin, F., Petit, J.-R., Raisbeck, G., Raynaud, D., Röthlisberger, R., Ruth, U., Rybak, O., Severi, M., Schmitt, J., Schwander, J., Siegenthaler, U., Siggaard-Andersen, M.-L., Spahni, R., Steffensen, J. P., Stenni, B., Stocker, T. F., Tison, J.-L., Traversi, R., Udisti, R., Valero-Delgado, F., van den Broeke, M. R., van de Wal, R. S. W., Wagenbach, D., Wegner, A., Weiler, K., Wilhelms, F., Winther, J.-G., and Wolff, E.: One-to-one coupling of glacial climate variability in Greenland and Antarctica, Nature, 444, 195–198, https://doi.org/10.1038/nature05301, 2006.

Fredriksen, H.-B. and Rypdal, K.: Spectral Characteristics of Instrumental and Climate Model Surface Temperatures, Journal of Climate, 29, 1253 – 1268, https://doi.org/10.1175/JCLI-D-15-0457.1, 2016.

Gkinis, V., Vinther, B. M., Popp, T. J., Faber, A.-K., Holme, C. T., Jensen, C. M., Lanzky, M., Lütt, A. M., Mandrakis, V., Ørum, N. O., Pedersen, A.-S., Vaxevani, N., Weng, Y., Capron, E., Dahl-Jensen, D., Hörhold, M., Jones, T. R., Jouzel, J., Landais, A., Masson-Delmotte, V., Oerter, H., Rasmussen, S. O., Steen-Larsen, H. C., Steffensen, J. P., Árný E Sveinbjörnsdottir, Vaughn, B. H., and White, J.: A 120,000-year long climate record from a NW-Greenland deep ice core at ultra-high resolution, https://doi.org/10.1038/s41597-021-00916-9, 2021.

Guo, Z. T., Berger, A., Yin, Q. Z., and Qin, L.: Strong asymmetry of hemispheric climates during MIS-13 inferred from correlating China loess and Antarctica ice records, Climate of the Past, 5, 21–31, https://doi.org/10.5194/cp-5-21-2009, 2009.

Hébert, R., Rehfeld, K., and Laepple, T.: Comparing estimation techniques for temporal scaling in palaeoclimate time series, Nonlinear Processes in Geophysics, 28, 311–328, https://doi.org/10.5194/npg-28-311-2021, 2021.

Huybers, P. and Curry, W.: Links between annual, Milankovitch and continuum temperature variability, Nature, 441, 329–332, https://doi.org/10.1038/nature04745, 2006.

https://doi.org/10.5194/egusphere-2023-1858
Preprint. Discussion started: 5 September 2023

Jouzel, J., Masson-Delmotte, V., Cattani, O., Dreyfus, G., Falourd, S., Hoffmann, G., Minster, B., Nouet, J., Barnola, J. M., Chappellaz, J., Fischer, H., Gallet, J. C., Johnsen, S., Leuenberger, M., Loulergue, L., Luethi, D., Oerter, H., Parrenin, F., Raisbeck, G., Raynaud, D., Schilt, A., Schwander, J., Selmo, E., Souchez, R., Spahni, R., Stauffer, B., Steffensen, J. P., Stenni, B., Stocker, T. F., Tison, J. L., Werner, M., and Wolff, E. W.: Orbital and Millennial Antarctic Climate Variability over the Past 800,000 Years, Science, 317, 793–796, https://doi.org/10.1126/science.1141038, 2007.

Laepple, T. and Huybers, P.: Reconciling discrepancies between Uk37 and Mg/Ca reconstructions of Holocene marine temperature variability, Earth and Planetary Science Letters, 375, 418–429, https://doi.org/https://doi.org/10.1016/j.epsl.2013.06.006, 2013.

Laepple, T. and Huybers, P.: Ocean surface temperature variability: Large model–data differences at decadal and longer periods, Proceedings of the National Academy of Sciences, 111, 16 682–16 687, https://doi.org/10.1073/pnas.1412077111, 2014.

Lambert, F., Delmonte, B., Petit, J. R., Bigler, M., Kaufmann, P. R., Hutterli, M. A., Stocker, T. F., Ruth, U., Steffensen, J. P., and Maggi, V.: Dust-climate couplings over the past 800,000 years from the EPICA Dome C ice core, Nature, 452, 616–619, https://doi.org/10.1038/nature06763, 2008.

Lambert, F., Bigler, M., Steffensen, J. P., Hutterli, M., and Fischer, H.: Centennial mineral dust variability in high-resolution ice core data from Dome C, Antarctica, Climate of the Past, 8, 609–623, https://doi.org/10.5194/cp-8-609-2012, 2012.

Lamy, F., Gersonde, R., Winckler, G., Esper, O., Jaeschke, A., Kuhn, G., Ullermann, J., Martinez-Garcia, A., Lambert, F., and Kilian, R.: Increased Dust Deposition in the Pacific Southern Ocean During Glacial Periods, Science, 343, 403–407, https://doi.org/10.1126/science.1245424, 2014.

Lovejoy, S.: A voyage through scales, a missing quadrillion and why the climate is not what you expect, Climate Dynamics, 44, 3187–3210, https://doi.org/10.1007/s00382-014-2324-0, 2015.

Lovejoy, S.: Review Article: Scaling, dynamical regimes and stratification: How long does weather last? How big is a cloud?, Nonlinear Processes in Geophysics Discussions, 2023, 1–146, https://doi.org/10.5194/npg-2023-5, 2023.

Lovejoy, S. and Lambert, F.: Spiky fluctuations and scaling in high-resolution EPICA ice core dust fluxes, Climate of the Past, 15, 1999–2017, https://doi.org/10.5194/cp-15-1999-2019, 2019.

Lovejoy, S. and Schertzer, D.: Haar wavelets, fluctuations and structure functions: convenient choices for geophysics, Nonlinear Processes in Geophysics, 19, 513–527, https://doi.org/10.5194/npg-19-513-2012, 2012.

Lovejoy, S. and Varotsos, C.: Scaling regimes and linear/nonlinear responses of last millennium climate to volcanic and solar forcings, Earth System Dynamics, 7, 133–150, https://doi.org/10.5194/esd-7-133-2016, 2016.

Lyle, M., Heusser, L., Ravelo, C., Andreasen, D., Olivarez Lyle, A., and Diffenbaugh, N.: Pleistocene water cycle and eastern boundary current processes along the California continental margin, Paleoceanography, 25, https://doi.org/10.1029/2009PA001836, 2010.

Markle, B., Steig, E., Roe, G., Winckler, G., and McConnell, J.: Concomitant variability in high-latitude aerosols, water isotopes and the hydrologic cycle, Nature Geoscience, 11, 853–859, https://doi.org/10.1038/s41561-018-0210-9, 2018.

Masson-Delmotte, V., Dreyfus, G., Braconnot, P., Johnsen, S., Jouzel, J., Kageyama, M., Landais, A., Loutre, M.-F., Nouet, J., Parrenin, F., Raynaud, D., Stenni, B., and Tuenter, E.: Past temperature reconstructions from deep ice cores: relevance for future climate change, Climate of the Past, 2, 145–165, https://doi.org/10.5194/cp-2-145-2006, 2006.

Nilsen, T., Rypdal, K., and Fredriksen, H.-B.: Are there multiple scaling regimes in Holocene temperature records?, Earth System Dynamics, 7, 419–439, https://doi.org/10.5194/esd-7-419-2016, 2016.

North Greenland Ice Core Project members, Andersen, K. K., Azuma, N., Barnola, J.-M., Bigler, M., Biscaye, P., Caillon, N., Chappellaz, J., Clausen, H. B., Dahl-Jensen, D., Fischer, H., Flückiger, J., Fritzsche, D., Fujii, Y., Goto-Azuma, K., Grønvold, K., Gundestrup, N. S.,

https://doi.org/10.5194/egusphere-2023-1858
Preprint. Discussion started: 5 September 2023

Hansson, M., Huber, C., Hvidberg, C. S., Johnsen, S. J., Jonsell, U., Jouzel, J., Kipfstuhl, S., Landais, A., Leuenberger, M., Lorrain, R., Masson-Delmotte, V., Miller, H., Motoyama, H., Narita, H., Popp, T., Rasmussen, S. O., Raynaud, D., Rothlisberger, R., Ruth, U., Samyn, D., Schwander, J., Shoji, H., Siggard-Andersen, M.-L., Steffensen, J. P., Stocker, T., Sveinbjörnsdóttir, A. E., Svensson, A., Takata, M., Tison, J.-L., Thorsteinsson, T., Watanabe, O., Wilhelms, F., and White, J. W. C.: High-resolution record of Northern Hemisphere climate extending into the last interglacial period, Nature, 431, 147–151, https://doi.org/10.1038/nature02805, 2004.

Petit, J. R., Jouzel, J., Raynaud, D., Barkov, N. I., Barnola, J.-M., Basile, I., Bender, M., Chappellaz, J., Davis, M., Delaygue, G., Delmotte, M., Kotlyakov, V. M., Legrand, M., Lipenkov, V. Y., Lorius, C., PÉpin, L., Ritz, C., Saltzman, E., and Stievenard, M.: Climate and atmospheric history of the past 420,000 years from the Vostok ice core, Antarctica, Nature, 399, 429–436, https://doi.org/10.1038/20859, 1999.

Reschke, M., Kröner, I., and Laepple, T.: Testing the consistency of Holocene and Last Glacial Maximum spatial correlations in temperature proxy records, Journal of Quaternary Science, 36, 20–28, https://doi.org/10.1002/jqs.3245, 2021.

Ruddiman, W.: Earth's Climate: Past and Future, W. H. Freeman, https://books.google.cl/books?id=n-Fv4vYIQcIC, 2008.

Ruth, U., Barnola, J.-M., Beer, J., Bigler, M., Blunier, T., Castellano, E., Fischer, H., Fundel, F., Huybrechts, P., Kaufmann, P., Kipfstuhl, S., Lambrecht, A., Morganti, A., Oerter, H., Parrenin, F., Rybak, O., Severi, M., Udisti, R., Wilhelms, F., and Wolff, E.: "EDML1": a chronology for the EPICA deep ice core from Dronning Maud Land, Antarctica, over the last 150 000 years, Climate of the Past, 3, 475–484, https://doi.org/10.5194/cp-3-475-2007, 2007a.

Ruth, U., Bigler, M., Röthlisberger, R., Siggaard-Andersen, M.-L., Kipfstuhl, S., Goto-Azuma, K., Hansson, M. E., Johnsen, S. J., Lu, H., and Steffensen, J. P.: Ice core evidence for a very tight link between North Atlantic and east Asian glacial climate, Geophysical Research Letters, 34, https://doi.org/https://doi.org/10.1029/2006GL027876, 2007b.

Sato, H., Suzuki, T., Hirabayashi, M., Iizuka, Y., Motoyama, H., and Fujii, Y.: Mineral and Sea-Salt Aerosol Fluxes over the Last 340 kyr Reconstructed from the Total Concentration of Al and Na in the Dome Fuji Ice Core, Atmospheric and Climate Sciences, 3, 186–192, https://doi.org/10.4236/acs.2013.32020, 2013.

Schüpbach, S., Federer, U., Kaufmann, P. R., Albani, S., Barbante, C., Stocker, T. F., and Fischer, H.: High-resolution mineral dust and sea ice proxy records from the Talos Dome ice core, Climate of the Past, 9, 2789–2807, https://doi.org/10.5194/cp-9-2789-2013, 2013.

Seierstad, I. K., Abbott, P. M., Bigler, M., Blunier, T., Bourne, A. J., Brook, E., Buchardt, S. L., Buizert, C., Clausen, H. B., Cook, E., Dahl-Jensen, D., Davies, S. M., Guillevic, M., Johnsen, S. J., Pedersen, D. S., Popp, T. J., Rasmussen, S. O., Severinghaus, J. P., Svensson, A., and Vinther, B. M.: Consistently dated records from the Greenland GRIP, GISP2 and NGRIP ice cores for the past 104 ka reveal regional millennial-scale δ18O gradients with possible Heinrich event imprint, Quaternary Science Reviews, 106, 29–46, https://doi.org/10.1016/j.quascirev.2014.10.032, 2014.

Simonsen, M., Baccolo, G., Blunier, T., Borunda, A., Delmonte, B., Frei, R., Goldstein, S., Grinsted, A., Kjær, H., Sowers, T., Svensson, A., Vinther, B., Vladimirova, D., Winckler, G., Winstrup, M., and Vallelonga, P.: East Greenland ice core dust record reveals timing of Greenland ice sheet advance and retreat, Nature Communications, 10, https://doi.org/10.1038/s41467-019-12546-2, 2019.

Tierney, J. E., Russell, J. M., Huang, Y., Damsté, J. S. S., Hopmans, E. C., and Cohen, A. S.: Northern Hemisphere Controls on Tropical Southeast African Climate During the Past 60,000 Years, Science, 322, 252–255, https://doi.org/10.1126/science.1160485, 2008.

von der Heydt, A. S., Ashwin, P., Camp, C. D., Crucifix, M., Dijkstra, H. A., Ditlevsen, P., and Lenton, T. M.: Quantification and interpretation of the climate variability record, Global and Planetary Change, 197, 103 399, https://doi.org/10.1016/j.gloplacha.2020.103399, 2021.

Wunsch, C.: The spectral description of climate change including the 100 ky energy, Climate Dynamics, 20, 353–363, https://doi.org/10.1007/s00382-002-0279-z, 2003.

https://doi.org/10.5194/egusphere-2023-1858
Preprint. Discussion started: 5 September 2023

Zhu, F., Emile-Geay, J., McKay, N. P., Hakim, G. J., Khider, D., Ault, T. R., Steig, E. J., Dee, S., and Kirchner, J. W.: Climate models
445 can correctly simulate the continuum of global-average temperature variability, Proceedings of the National Academy of Sciences, 116, 8728–8733, https://doi.org/10.1073/pnas.1809959116, 2019.